

See discussions, stats, and author profiles for this publication at: <https://www.researchgate.net/publication/5633508>

Single-Coil, Multisample, Proton Relaxation Method for Magnetic Relaxation Switch Assays

ARTICLE *in* ANALYTICAL CHEMISTRY · MARCH 2008

Impact Factor: 5.64 · DOI: 10.1021/ac702288r · Source: PubMed

CITATIONS

24

READS

60

5 AUTHORS, INCLUDING:



Pablo Prado

One Resonance Sensors, LLC

37 PUBLICATIONS 571 CITATIONS

SEE PROFILE

Single-Coil, Multisample, Proton Relaxation Method for Magnetic Relaxation Switch Assays

Thomas J. Lowery,* Robert Palazzolo, Susanna M. Wong, Pablo J. Prado, and Sonia Taktak

T2 Biosystems, 286 Cardinal Medeiros Avenue, Cambridge, Massachusetts 02141

Nanoparticle based magnetic relaxation switch (MRSw) biosensors offer the opportunity to develop magnetic resonance based in vitro diagnostics. Critical attributes for point of care in vitro diagnostic products include simple instrumentation and ease of use. To this end, high-resolution biexponential analysis was used to permit measurement and assignment of two samples with a single radio frequency detection coil. This approach was used to calibrate and expand the dynamic range of MRSw biosensors in a single step. The potential for easy-to-use MRSw-based diagnostics was demonstrated by combining the method for single-step measurement of two samples with a disposable, plastic cartridge and dried MRSw reagents to obtain a calibrated reading after only two steps: mix and read. Taken together, our results suggest the feasibility of developing magnetic resonance based in vitro diagnostics that offer extreme ease of use and simple instrumentation.

Magnetic resonance (MR) is an established technology for medical diagnostics. To date, MR diagnostics have been primarily limited to in vivo studies using high-field, stationary magnetic resonance imaging (MRI) scanners. Inherent limitations in sensitivity and selectivity have precluded widespread use of MR for in vitro diagnostics (IVD), which typically requires analysis of small volumes (less than a milliliter) of body fluids in a highly sensitive, selective, and rapid fashion. However, these limitations appear to be surmountable since the advent of superparamagnetic nanoparticle based biosensors, known as magnetic relaxation switches (MRSw).¹

Recently, MRSw has been used for detecting biomolecules in homogeneous assays and has demonstrated low sensitivities, in the picomolar range for nucleic acids and proteins^{2,4} and five viral particles in 10 μL .⁶ The wide variety of target analytes that have

been detected using this approach include small molecules, nucleic acids, bacterial cells, proteins, enzymes, and viruses.^{2–6} Typically, MRSw assays are configured such that the presence of analyte induces the nanoparticles to transition from a dispersed state to a clustered state (Figure 1). This transition occurs because the nanoparticles, which are ~ 30 nm in diameter, have been sensitized to the presence of analyte by surface decoration with an appropriate binding agent. When in the presence of a magnetic field, microscopic field nonuniformities are created due to the formation of induced magnetic dipoles in the superparamagnetic nanoparticles. These nonuniformities in the magnetic field cause spin dephasing of ^1H nuclei of water, which leads to a time-dependent decrease in the ^1H signal during detection by a radio frequency pulse sequence.⁴ The resulting exponential relaxation curve decays according to a time constant known as T_2 , which depends linearly upon analyte concentration.

A promising attribute of MRSw assays is the potential to probe “dirty”, nonoptical samples, such as blood,^{5,7} cell culture media,⁸ and milk.⁵ The ability to work with nonoptical samples may eliminate time-consuming and complex processing steps associated with conventional optical applications. In contrast, MRSw diagnostics could be used in a simple fashion relative to other in vitro diagnostic tests. Although the potential for single-step measurements has been recognized, T_2 variations between samples have always necessitated measurement of the test sample and at least one reference sample to obtain calibrated results. To date, this has been achieved by either making sequential measurements with a relaxometer or by obtaining a T_2 -weighted image with an MRI scanner. The cost and requisite technical expertise make MRI scanners unsuitable instruments for routine in vitro diagnostics measurements; therefore, a simpler, more affordable alternative is needed to realize the potential of single-step measurements for MRSw diagnostics. Preferably instruments with a single detection coil and no additional hardware could be utilized for this purpose. Here we present a signal acquisition method for obtaining T_2 values for more than one sample inside of a single radio frequency (rf) detection coil and demonstrate how this method enables two types of validated single-step measurements. We also present how single-step measurements can be obtained with a reconstituted dried nanoparticle formulation in a disposable cartridge to allow the user to

* To whom correspondence should be addressed. Phone: 617-661-8282 ext 223. Fax: 617-876-1608. E-mail: tlowery@t2biosystems.com.

(1) Josephson, L.; Perez, L. M.; Weissleder, R. *Angew. Chem., Int. Ed.* **2001**, *40*, 3204–3206.

(2) Perez, J. M.; Josephson, L.; O’Loughlin, T.; Hogemann, D.; Weissleder, R. *Nature Biotechnol.* **2002**, *20*, 816–820.

(3) Tsourkas, A.; Hofstetter, O.; Hofstetter, H.; Weissleder, R.; Josephson, L. *Angew. Chem., Int. Ed.* **2004**, *43*, 2395–2399.

(4) Perez, J. M.; Josephson, L.; Weissleder, R. *ChemBioChem* **2004**, *5*, 261–264.

(5) Kaittanis, C.; Naser, S. A.; Perez, J. M. *Nano Lett.* **2007**, *7*, 380–383.

(6) Perez, J. M.; Simeone, F. J.; Saeki, Y.; Josephson, L.; Weissleder, R. *J. Am. Chem. Soc.* **2003**, *125*, 10192–10193.

(7) Zhao, M.; Josephson, L.; Tang, Y.; Weissleder, R. *Angew. Chem., Int. Ed.* **2003**, *42*, 1375–1378.

(8) Harris, T. J.; von Maltzahn, G.; Derfus, A. M.; Ruoslahti, E.; Bhatia, S. N. *Angew. Chem., Int. Ed.* **2006**, *45*, 3161–3165.

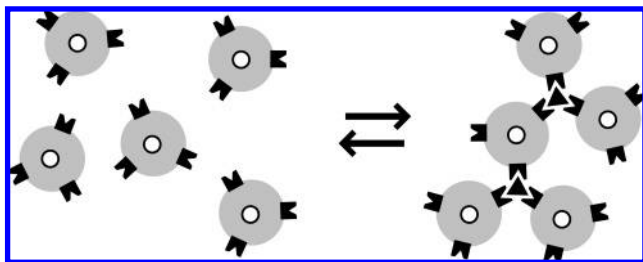


Figure 1. Magnetic relaxation switches detect analyte (black triangles) by transitioning between a dispersed state and clustered state in the presence of analyte. The nanoparticles (30 nm DIA) consist of a monocrystalline iron oxide core (white circles) with a cross-linked dextran coating (gray circles) and attached moieties (black) that selectively bind the desired analyte (black triangles). Nanoparticle clustering leads to a decrease in the T_2 relaxation signal.

acquire a validated diagnostic result in two easy steps: fluid addition and measurement.

Theoretical Basis. Because relaxation curves for homogeneous MRSw nanoparticle solutions are monoexponential,¹⁴ the acquired signal from n samples in different containers within a single detection coil is the sum of n monoexponential curves according to the equation

$$y(t) = \sum_{i=1,2,\dots,n} \text{Amp}(i) \exp[-t/T_2(i)] + \text{Offset} \quad (1)$$

where $y(t)$ is the signal amplitude as a function of time, t ; n is the number of samples; $\text{Amp}(i)$ and $T_2(i)$ are the amplitude and T_2 decay constant for the i th sample; and Offset is the signal offset. When considered in light of eq 1, the problem of multiple sample detection is essentially a problem of multiexponential analysis. A plethora of methods exist for extracting $\text{Amp}(i)$ and $T_2(i)$ from $y(t)$;⁹ however, accurate results rely upon selecting the method best suited for the underlying scenario yielding the multiexponential behavior. Existing methods for analyzing discrete sums of exponential decay curves, which have been optimized for identifying the number of components (i) and sampling a large parameter space of possible fit coefficient values,^{10–12} are not well suited for MRSw assays where the number of components and the possible range of T_2 and amplitude values are dictated by assay configuration. As will be shown below, the two most critical attributes for MRSw assay exponential analysis, which are high accuracy and the absence of false positives, can be adequately addressed by a tailored method for exponential analysis.

Low accuracy and unreliability for closely spaced decay constants is a well understood limitation of exponential analysis.¹⁰ Two previous studies using multiexponential analysis for discriminating T_2 relaxation constants report resolution of T_2 values at ratios of 2.5 and 1.6.^{13,14} These results are not inconsistent with

each other as the resolution of exponential relaxation rates is determined by the signal-to-noise ratio (SNR) and the domain of the possible decay constants.^{9,15} For the SNR obtained in this study (120), the maximum resolution for an infinite domain is 2.37.^{9,15} Although maximal resolution does improve with domain size, improvement is not significant until the domain approaches 10^1 .¹⁵ Poor resolution is not the only limitation of multiexponential analysis. When the difference in decay constants is below the limit of resolution, the output results become unreliable,⁹ which could lead to false positives or false negatives if used for medical diagnostics.

EXPERIMENTAL SECTION

MR Relaxometry. All experiments were conducted on a Bruker MiniSpec (The Woodlands, TX) mq20 relaxometer operating at 0.47 T (19.95 MHz) and 40 °C. Samples were incubated in the instrument for at least 5 min to ensure temperature equilibration. CPMG pulse sequences with an interecho delay of 0.5 ms, eight scans, 3000 echos, and a recycle delay of 2 s were used. The sampling time was selected to be at least five times the longest T_2 value for artifact-free fitting. It is believed that the high SNR for low filling factors likely resulted from the high homogeneity of the magnetic field (< 20 ppm).

Fabrication and Detection Inside the Plastic Container.

A plastic sample cartridge containing two chambers was machined from Delrin (polyoxymethylene) to hold two sample volumes (120 and 240 μL) inside the detection region of the Bruker minispec 10 mm diameter radio frequency coil (Figure 2). The minimal sample volume of each chamber was determined by measuring the signal amplitude as a function of volume. Typically, containers for MR analysis are made of glass or a material that does not contain the nucleus being detected. Although Delrin is a hydrogen-rich substance, selective relaxation measurements of the liquid sample inside of the delrin container are feasible due to the significant difference between the characteristics of the Delrin and liquid signals. This demonstration shows the possibility of using common materials and technologies for fabricating cheap, disposable sample containers.

Exponential Fitting. All curve fits were executed using custom scripts in MATLAB (The Mathworks, Natick, MA). For all fits, T_2 coefficients were constrained between 0 and 1000 ms and the amplitude values between 0 and 100. The maximum number of evaluations and iterations were 1000, and the fit algorithm was the MATLAB default using the “trust region” algorithm. For data shown in Figures 3–6, start values of 40% for the amplitudes, 20 and 115 ms for the T_2 values of the large and small chambers, and 0.5 for the offset were used. Unlike for eq 2, fit results for eq 3 depended on the initial T_2 values used, which is not uncommon for nonlinear least-squares analysis; for example, if the initial values were reversed, the T_2 coefficients were less accurate. This likely arose from the T_2 values being assigned to relative amplitudes in eq 3 and the fitting algorithm stalling in a local minimum, but as the data show, accurate results can be obtained using starting values appropriately tailored to the assay configuration.

(9) Istratov, A. A.; Vyvenko, O. F. *Rev. Sci. Instrum.* **1999**, *70*, 1233–1257.

(10) Whittal, K. P.; MacKay, A. L. *J. Magn. Reson.* **1989**, *84*, 134–152.

(11) Provencher, S. W. *Biophys. J.* **1976**, *16*, 27–41.

(12) Provencher, S. W. *J. Chem. Phys.* **1976**, *64*, 2772–2777.

(13) Fransson, A.; Ericsson, A.; Jung, B.; Henriksson, U. *Phys. Med. Biol.* **1989**, *34*, 305–314.

(14) Lupu, M.; Todor, D. *Chemom. Intell. Lab. Syst.* **1995**, *29*, 11–17.

(15) Bertero, M.; Boccacci, P.; Pike, E. R. *Proc. R. Soc. London, Ser. A* **1982**, *383*, 15–29.

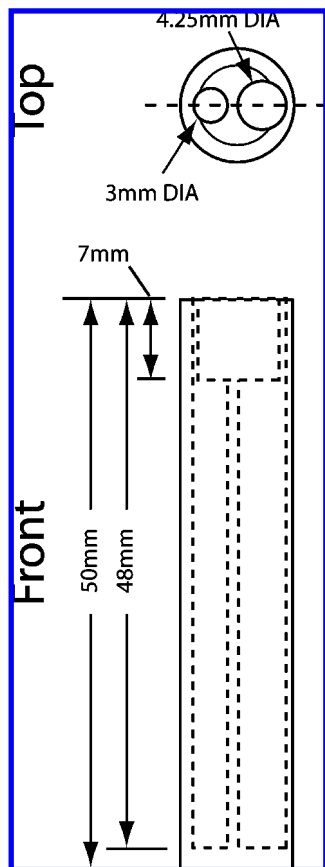


Figure 2. Schematic of the plastic two-chamber sample cartridge. Delrin rod (10 mm o.d. \times 50 mm long) with two sample chambers (3 mm and 4.25 mm i.d. \times 48 mm deep) and female threads (7 mm deep) for attachment to a threaded sample holder for convenient insertion and removal from the relaxometer.

Model Systems. Signal acquisition and processing was developed and tested using CuSO_4 solutions ($1/T_1 = 3.20 \text{ (mg/mL)}^{-1} \text{ s}^{-1}$, $1/T_2 = 3.25 \text{ (mg/mL)}^{-1} \text{ s}^{-1}$ measured at 0.47 T). All MRSw demonstrations were conducted using biotinylated or SIA-coated nanoparticles ($1/T_1 = 25 \text{ mM}^{-1} \text{ s}^{-1}$, $1/T_2 = 48 \text{ mM}^{-1} \text{ s}^{-1}$ measured at 0.47 T). These were cross-linked, dextran-coated iron oxide nanoparticles prepared by colloidal synthesis. Surface modification of the parent aminated particles was performed using standard *N*-hydroxysuccinimide ester chemistry, as described in ref 16. Biotinylation was performed using the *N*-hydroxysuccinimide ester of biotin, (D-biotin-SE, from Invitrogen Carlsbad, CA) at a 1:1 ratio with *N*-succinimidyl iodacetate (SIA, from Molecular Biosciences, Boulder, CO) to yield about 100 biotin per nanoparticle, or 2000 Fe atoms, as previously described.¹⁶ SIA capped particles (control particles) were prepared the same way using SIA alone. The biotinylated and SIA-coated nanoparticles had diameters of 27 nm as determined by photon correlation light scattering using a Zetasizer 1000HS (Malvern Instruments, Marlboro, MA).

Avidin Titrations. Biotinylated nanoparticles were reacted with avidin in 10 mM PBS, 0.1 mg/mL BSA, pH 7.4 buffer. Reactions were allowed to incubate for at least 5 min at room

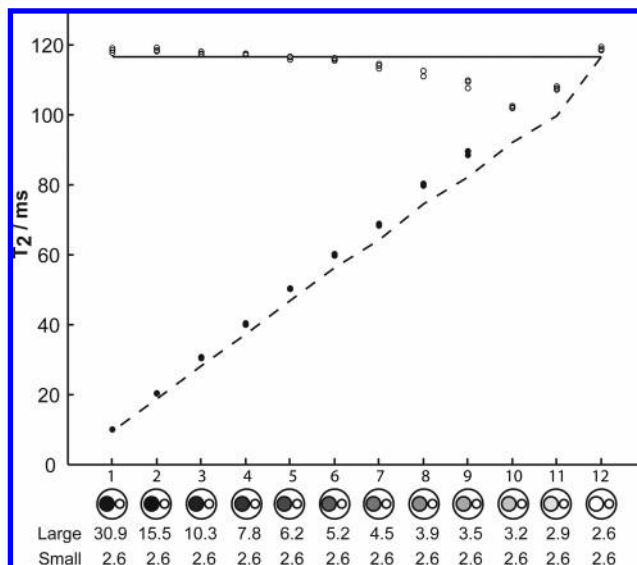


Figure 3. Plots of T_2 fit coefficients obtained for a series of CuSO_4 standard solutions. The small chamber of the plastic cartridge was filled with 2.6 mg/mL CuSO_4 , and the large chamber was filled with CuSO_4 solutions ranging in concentration from 30.9 to 2.6 mg/mL. T_2 values of these solutions were first obtained individually and were plotted for the large (—) and small (—) chambers. Fitting relaxation curves obtained from both chambers simultaneously with eq 3 resulted in the T_2 coefficients for the small (○) and large (●) chambers following the same trend as the actual values for concentrations 30.9–3.5 mg/mL CuSO_4 . All data were acquired, analyzed, and plotted in triplicate.

temperature prior to measurement. The maximum T_2 switch was observed for 1.5 μM avidin using an iron concentration of 0.075 mM (or 40 avidin per 2000 Fe).

Dry Formulation. Biotinylated coated nanoparticle solution (216 μL , 0.083 mM Fe, 10 mM PBS, 20 mg/mL dextran, pH 7.4) was placed into a 3.4 mm glass tube, and SIA-coated nanoparticle solution (108 μL , 0.083 mM Fe, 10 mM PBS, 20 mg/mL dextran, pH 7.4) was placed into a 2.4 mm glass tube. The tubes were frozen at -80°C and placed in a VirTis freeze dryer (Gardiner, NY) for 24 h. The dried biotinylated reagent was transferred into the larger sample chamber, and the dried SIA-coated reagent was transferred into the smaller sample chamber. Reconstitution medium (1.5 μM avidin in 1 mM PBS and 0.1 mg/mL BSA) was pipetted into the dried reagents, 240 μL for the biotinylated and 120 μL for the SIA-coated.

RESULTS AND DISCUSSION

The possibility for extracting reliable, high-resolution T_2 values from multiexponential relaxation curves was assessed using the simplest case of measuring only two samples within a single rf coil. Biexponential relaxation curves were obtained from a series of 12 combinations of CuSO_4 solutions inside of the two-chamber cartridge. These 12 combinations were chosen to adequately sample a range of T_2 combinations representative of MRSw biosensors. For all sample combinations, the smaller chamber contained a concentration of 2.6 mg/mL CuSO_4 ($T_2 = 117 \pm 1$ ms) and the larger chamber contained CuSO_4 concentrations ranging between 30.6 and 2.6 mg/mL ($T_2 = 10 \pm 1$ ms to $T_2 = 117 \pm 1$ ms). Relaxation curves were obtained for the solutions

(16) Taktak, S.; Sosnovik, D.; Cima, M. J.; Weissleder, R.; Josephson, L. *Anal. Chem.* **2007**, *79*, 8863–8869.

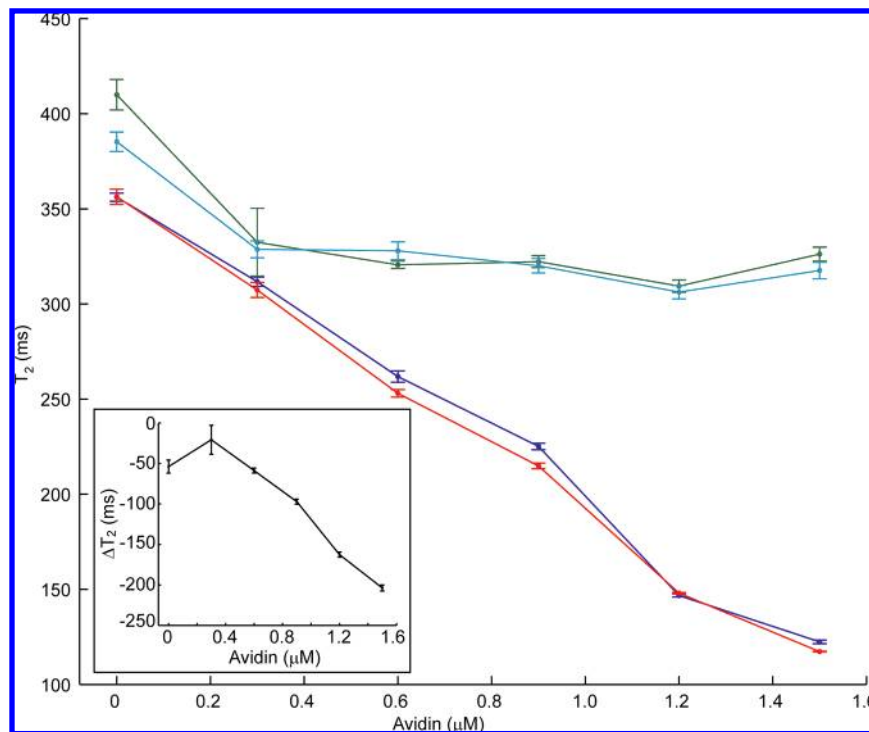


Figure 4. Demonstration of simultaneous acquisition of test and reference assays. Biotin-free nanoparticles (green and cyan) and biotinylated nanoparticles (red and blue) were titrated with increasing amounts of avidin inside of the two chamber cartridge. T_2 values from the small chamber containing biotin-free particles showed a small avidin-induced T_2 change, likely due to nonspecific binding, whereas values for the large chamber containing biotinylated particles showed a large linear response due to addition of avidin. Data obtained from simultaneous measurements and subsequent analyses using eq 3 for biotin-free (cyan) and biotinylated (blue) nanoparticles matches data obtained for individual measurements for biotin-free (green) and biotinylated (red) nanoparticles. The difference between the test and reference assays can serve as a calibration curve for obtaining validated results, because ΔT_2 can be correlated with the concentration of avidin (inset). Average values and standard deviations for triplicate measurements are shown by ● and error bars, respectively.

independently and in the combinations listed, Figure 3. For this scenario the detected signal is

$$y(t) = \text{Amp}(A) \exp[-t/T_2(A)] + \text{Amp}(B) \exp[-t/T_2(B)] + \text{Offset} \quad (2)$$

where coefficients A and B correspond to the values for the large and the small chambers. Constrained nonlinear least-squares (CNLS) fitting was conducted on this data set using eq 2. Although the accuracy of the results is somewhat compromised, the resolution is a T_2 ratio of ~ 2.5 , Figure S-1 of the Supporting Information. This is slightly larger than the theoretical maximal resolution.¹⁵ The similarity of the output values for sample combinations less than and greater than sample 7 shows that the output values of this method can be redundant, which would lead to false positives or false negatives if applied to MRSw signal processing. Other common methods of biexponential analysis were tested, such as DISCRETE,^{11–12} and yielded similar undesirable results (data not shown).

For each chamber, the amplitude coefficients should be proportional to the volume of solution inside the sensitive region of the detection coil, which was not the case for eq 2, Figure S-2. Therefore, the relative amplitudes of $\text{Amp}(A)$ and $\text{Amp}(B)$ can be constrained based on the known relative sensitive volumes of the two chambers. Additionally, the volume ratio of $\sim 2:1$ between the large and small chambers allows for the T_2 coefficients to be

assigned to their appropriate chamber. These modifications can be incorporated into eq 2 to yield

$$y(t) = \text{Amp} \exp[-t/T_2(A)] + 0.44 \text{ Amp} \exp[-t/T_2(B)] + \text{Offset} \quad (3)$$

where Amp corresponds to the amplitude for the larger chamber and 0.44 Amp corresponds to that for the smaller chamber. The absolute ratio of the two chambers (0.44) was determined by obtaining their signal amplitudes independently.

The same data set used in Figure S-1 was analyzed with eq 3 using identical fitting constraints to yield the results shown in Figure 3. Constraining the relative amplitudes in this manner yielded much greater accuracy over the complete range of T_2 values sampled and demonstrated the absence of redundancy in output values. As the T_2 values approach the limit of resolution, there is a small, seemingly linear deviation from the actual values until the fit values coalesce for sample combination 10 (92 ± 1 and 117 ± 1 ms). This indicates that the resolution of this method is ~ 1.3 , which is 1.8 times better than the theoretical limit. Achieving better resolution than theoretically predicted arises from fixing the absolute ratio of the amplitude coefficients, which decreases the number of coefficients and narrows the set of possible solutions. Even higher resolution should be possible by achieving a higher SNR than 120 by increasing the filling factor of the detection coil beyond its current value (27% for both

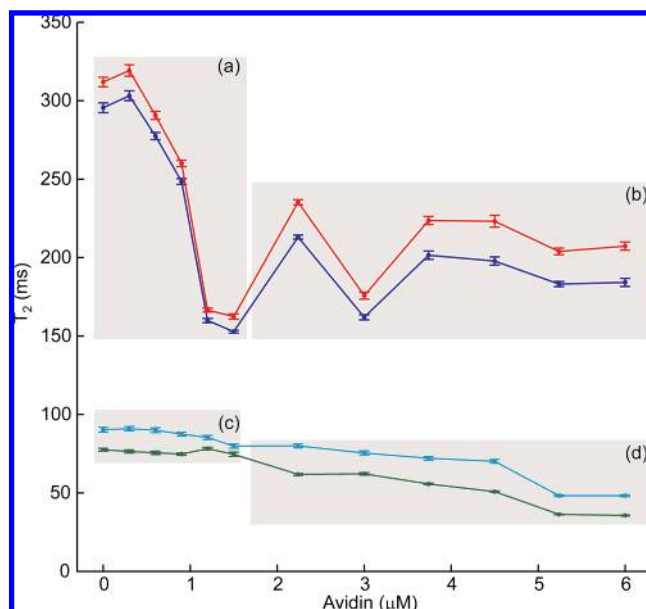


Figure 5. Demonstration of simultaneous detection of two different nanoparticle concentrations to control for prozoning and expand the dynamic range of a single measurement. Independent measurements of both 0.075 mM Fe biotin-CLIO (red) and 0.25 mM Fe biotin-CLIO (cyan) over a range of avidin concentrations show that the lower concentration assay (red) has a steep, linear T_2 response below 1.5 μM avidin and erratic T_2 values above 1.5 μM avidin due to overtitration. The higher concentration assay (cyan) shows a moderate T_2 response over a broader concentration of avidin. The lower (blue) and higher (green) concentration assays were simultaneously measured in the large and small chambers of the plastic cartridge, respectively. Subsequent analysis with eq 3 demonstrates that both assays can be sampled simultaneously. Although there is a downward, seemingly systematic shift in the T_2 values detected simultaneously, determining whether the T_2 of the higher concentration assay is in region c or d still allows for the unambiguous determination of whether the T_2 of the lower concentration assay corresponds to region a or b. For example, T_2 values of 200 and 85 ms indicate a concentration below 1.5 μM , while T_2 values of 200 and 60 ms indicate a concentration above 1.5 μM . Average values and standard deviations for triplicate measurements are shown by \bullet and error bars, respectively.

chambers filled) or by signal averaging. Although the possibility remains for increasing the number of samples by extending eq 3, it will be increasingly challenging without significant increase in the SNR and application to specific scenarios where the range of possible T_2 values for each sample does not significantly overlap. Otherwise, quality would be compromised due to a loss of resolution.

Single-Step, Calibrated Measurements. The utility of eq 3 for MRSw diagnostics was demonstrated using a biotin/avidin model system, which displays the analyte-induced T_2 -response of a typical MRSw diagnostic, as previously described.¹⁶ This first example demonstrates how a reference and test sample can be measured simultaneously to obtain a calibrated T_2 measurement. In this case, the reference sample controls for nonspecific aggregation of nanoparticles, which can lead to false positives. This example addresses false positives as they are commonly observed for MRSw due to nonspecific aggregation. A similar approach using a different reference assay could be used to control for false negatives. The reference and test samples consisted of biotin-free nanoparticles and biotinylated nanoparticles, respec-

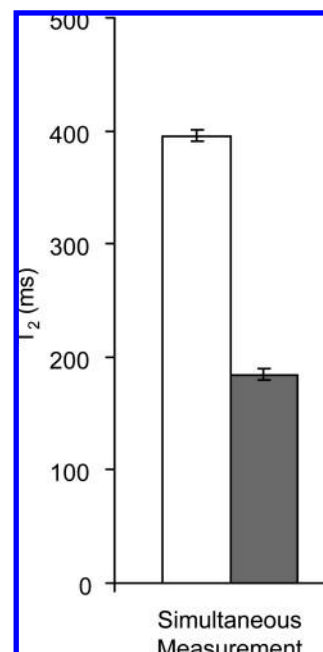


Figure 6. Demonstration of a single-step diagnostic assay. A solution of 1.5 μM avidin was added to dried formulations of biotin-free nanoparticles (white columns) and biotinylated nanoparticles (gray columns) inside a plastic cartridge. The difference in T_2 values (~ 200 ms) obtained from simultaneous measurement is similar to that obtained for particles that were not dried (Figure 2 inset). Error bars were calculated from triplicate measurements of a single sample.

tively. Increasing concentrations (0–1.5 μM) of avidin were added to the reference and test samples resulting in the T_2 of the reference sample decreasing in a nonlinear fashion from 385 ± 5 to 306 ± 5 ms, which likely resulted from nonspecific binding, and the test sample decreasing in a linear fashion from 356 ± 5 to 109 ± 1 ms (Figure 4). Obtaining signal from the reference and test solutions simultaneously and analyzing the data using eq 3 resulted in T_2 values that closely match those obtained from the samples independently (Figure 4). The T_2 values can be assigned to the appropriate chambers because of the ratio of amplitudes, which were 50.4% and 22.2%, and the difference between the T_2 values for each sample can be plotted as a function of analyte concentration to demonstrate the dynamic range of the assay (Figure 4, inset).

Single-Step, Increased Dynamic Range Measurements.

Another attribute of MRSw assays that requires sample calibration is that of overtitrating the nanoparticles with analyte. As has been previously shown, when analyte concentrations are higher than the optimal range of an MRSw assay, the measured T_2 is no longer correlated with the actual concentration of analyte.¹⁶ For example, when avidin is added beyond the linear range of a given particle concentration, the T_2 values begin to increase and respond in a manner that is uncorrelated with analyte concentration (Figure S-3). This effect, which has been compared to the prozone effect observed in other diagnostic tests, has been shown to arise from the clusters becoming unstable in solution.^{16,17} Although this condition can be detected by calculating the standard deviation of three T_2 measurements spaced by several minutes or by

(17) Kim, G.; Joesphson, L.; Langer, R.; Cima, M. *Bioconj. Chem.* **2007**, *18*, 2024–2028.

measuring the T_1 of the sample, both approaches require a significant amount of additional time and both require further analyses to determine the actual concentration of analyte. Therefore, neither is ideal for simple, easy-to-use, single-step diagnostic measurements, especially because both methods require either sample dilution or nanoparticle addition to determine the actual concentration of analyte.¹⁶

Here we demonstrate how single-step measurement and analysis with eq 3 can not only detect overtitation but also how it can be used to expand the effective dynamic range of MRSw tests. Because the sensitive region of an MRSw assay depends on nanoparticle concentration,¹⁶ a wider concentration range of avidin than any single assay can be detected in a single step fashion by simultaneously detecting the response of two nanoparticle concentrations to the same analyte solution. Changing the nanoparticle concentration affects not only the sensitive region of an assay but it also affects its slope. For example, the avidin-sensitive region for a concentration of 0.075 mM Fe biotinylated nanoparticles is between 0 and 1.5 μ M where the T_2 decreases by 150 ms; at higher avidin concentrations the T_2 values increase and become erratic (Figure 5). For nanoparticle concentrations of 0.25 mM, the T_2 response is only 30 ms over an avidin concentration of 6 μ M (Figure 5). Lower concentrations of nanoparticles have greater sensitivity (steeper response slopes) but narrow dynamic ranges (Figure 5a), and higher concentrations of nanoparticles have lower sensitivity (more gradual slopes) and broader dynamic ranges (Figure 5c,d). Measurement of the same analyte solution with both assays allows one to obtain high sensitivity for low analyte concentrations while maintaining adequate sensitivity for higher concentrations of analyte.

This method was demonstrated by adding increasing amounts of avidin (0–6 μ M) to low (0.075 mM Fe) and high (0.25 mM Fe) concentration solutions of biotinylated nanoparticles inside of the large and small chambers of the plastic cartridge, respectively. The T_2 values obtained using eq 3 and CNNLS follow the same trend as the actual T_2 values. Given an unknown concentration of avidin and the T_2 values for both concentrations of nanoparticles, the curves in Figure 5 can be used to calculate the avidin concentration as follows: (1) If the T_2 value of the concentrated nanoparticle chamber lies within region c (Figure 5) then the curve in region a (Figure 5) would be used to calculate the avidin concentration from the T_2 value of the dilute nanoparticle chamber. (2) If the T_2 value of the concentrated nanoparticle chamber lies within region d (Figure 5) then the curve in region d would be used to calculate the avidin concentration from T_2 value of the concentrated nanoparticle chamber. This avoids miscalculation that would arise from using region b (Figure 5) for calibration. Overtitration of the concentrated nanoparticle chamber may need to be detected by using the method of T_1 measurement previously proposed.¹⁶ As the dose response of the biotin/avidin system presented here is not highly sensitive, this example is meant to only demonstrate the concept behind enhancing the dynamic range of an MRSw assay. The actual

magnitude of enhancement will depend on the dose response for each MRSw assay to analyte and nanoparticle concentrations.

Single-Step Measurements with a Dried Reagent. The preceding examples of calibrated measurements and dynamic range expansion only address making more than one T_2 measurement in a single step. To demonstrate the potential for simple to use MRSw diagnostics, solutions of biotin-free and biotinylated nanoparticles were freeze-dried and transferred into the plastic cartridge, after which the dried formulations were reconstituted with a buffered avidin solution to a final avidin concentration of 1.5 μ M. Analysis of the biexponential relaxation curves with eq 3 indicated that the difference between the T_2 values for the small and large chambers (Figure 6) is comparable to that obtained for particles that were not dried (Figure 4 inset). The absolute T_2 values of the reconstituted solutions are slightly higher than native solutions, which may be due to an effect of freeze drying or sample transfer. Process and fluidic optimization is underway to minimize such errors and to make liquid addition simple and easy to use, both of which will be reported in greater detail elsewhere.

CONCLUSION

Here we demonstrate methods that significantly improve the performance of MRSw diagnostics and enable single step “mix and read” capability. The sampling capability of the simplest MR hardware has been increased by a tailored method for high-resolution, biexponential analysis. This method allows for obtaining calibrated results in a single-step measurement by simultaneous acquisition of T_2 values from a reference and test sample; it also allows for the dynamic range expansion by simultaneous acquisition of T_2 values from solutions of different nanoparticle concentrations. This method can be used to increase the number of samples detected per coil on instrumentation that has one or more coils. We anticipate that this method along with dry formulations of MRSw diagnostics and the potential to make measurements inside disposable plastics will be instrumental in making cheap, simple, and easy-to-use MR-based in vitro diagnostics.

ACKNOWLEDGMENT

This work was funded by T2 Biosystems. The authors thank Doug Levinson, Jim Koziarz, and Lee Josephson for helpful discussions and the T2 Team for support.

SUPPORTING INFORMATION AVAILABLE

Plots for coefficient and amplitude values for CNNLS fits, MRSw biotin/avidin assays, and example exponential relaxation curve data with corresponding fits. This material is available free of charge via the Internet at <http://pubs.acs.org>.

Received for review November 5, 2007. Accepted December 10, 2007.

AC702288R